Evaluation of combined reference frame transformation for interturn fault detection in permanent-magnet multiphase machines

Evaluation of Combined Reference Frame Transformation for Interturn Fault Detection in Permanent-Magnet Multiphase Machines

Fabio Immovilli, *Member, IEEE*, Claudio Bianchini, *Member, IEEE*, Emilio Lorenzani, *Member, IEEE*, Alberto Bellini, *Member, IEEE*, and Emanuele Fornasiero

***Abstract*—This paper focuses on modeling and experimental validation of a diagnostic fault classification procedure for interturn fault detection in permanent-magnet (PM) multiphase machines designed for fault-tolerant electric drives. The diagnostic procedure is based on the symmetrical component theory and relies upon the combined space vector $\vec{D}$ that gathers information from the two original space vectors obtained with different reference frames. The diagnostic index effectiveness and robustness were also investigated against other fault types such as rotor eccentricities and magnet damage to assess its discrimination capability. The proposed procedure was experimentally evaluated for the interturn fault case on a five-phase PM machine. Experiments were carried out at different speed and load levels, with increasing numbers of short-circuited turns. Both simulation and experimental results demonstrated the feasibility of the proposed diagnostic method.**

***Index Terms*—AC machines, brushless machines, brushless motors, condition monitoring, electric machines, electrical fault detection, fault detection, fault diagnosis, fault tolerance, generators, multiphase machines, permanent-magnet (PM) machines, PM motors.**

NOMENCLATURE

$\vec{v}_{\alpha\beta}$	Voltage space vector in $\alpha\beta$ reference frame.
$\vec{v}_{\alpha 2\beta 2}$	Voltage space vector in $\alpha 2\beta 2$ reference frame.
$\vec{D}$	Combined reference frame space vector.
D_0	DC component of the combined reference frame space vector.
f_s	Supply frequency fundamental harmonic.
κ	Voltage reduction factor.
$2p$	Number of poles of the machine.
$\dot{a}$	Complex exponential used for reference frame quantities transformation.
K	Reference frame quantities transformation coefficient.
ν	Harmonic order index value.

Manuscript received February 2, 2014; revised April 30, 2014 and June 13, 2014; accepted July 14, 2014. This work was developed in the framework of PRIN2009 project "High Reliability Multi-Phase Electric Drives for the More Electric Aircraft," which was co-supported by the Italian Ministry of Research (MIUR).

F. Immovilli, C. Bianchini, and E. Lorenzani are with the Dipartimento di Scienze e Metodi dell'Ingegneria (DISMI), University of Modena and Reggio Emilia, 42122 Reggio Emilia, Italy (e-mail: fabio.immovilli@unimore.it).

A. Bellini is with the Department of Electrical, Electronic and Information Engineering (DEI), University of Bologna, 40126 Bologna, Italy.

E. Fornasiero is with the Department of Electrical Engineering (DIE), University of Padova, 35131 Padua, Italy.

Color versions of one or more of the figures in this paper are available online at http://ieeexplore.ieee.org.

Digital Object Identifier 10.1109/TIE.2014.2348945

I. INTRODUCTION

MULTIPHASE machines can introduce an improvement in the area of medium- to high-power drives. Compared with traditional three-phase drives, multiphase machines exhibit higher efficiency, torque-to-weight ratio, and torque-to-volume ratio [1], [2]. For a given voltage and power, increasing the number of phases implies a reduction in the current per phase and, therefore, the power rating of the switches. Their use is increasing in those applications where fault-tolerance and continuous operation is a mandatory request, such as in traction and aerospace applications [3], as well as a few industrial applications, where fault-tolerant operation is appreciated [4].

Multiphase machines are inherently fault tolerant as they can be designed to reduce the fault probability and to maintain operation in the presence of faults [5], [6].

A number of phases higher than three introduce a sort of redundancy in the system, i.e., in the electrical circuit and the control system. In fact, a multiphase machine offers several degrees of freedom that can be used to enhance the reliability of the drive [7]–[9], provided that electrical and mechanical fault diagnosis techniques are available. The multiphase drive can continue to operate smoothly in the event of certain faults such as the loss of one or more phases, maintaining control capabilities at the expense of a reduced torque [10].

Fault diagnosis techniques are an extensively investigated topic for three-phase electric machines, with the main purpose of early stage fault detection to conduct predictive maintenance and avoid loss of production or hazardous situations [11]–[13]. Especially for the three-phase induction motor, given its widespread use in the industry, extensive literature works exist on mechanical fault detection, such as bearings [14], [15] and rotor eccentricity [16]. Other publications dealt with eccentricity in permanent-magnet (PM) synchronous machines by means of analytical methods, [17], [18] or finite-element (FE) analysis [19], [20].

Faults on multiphase machines are similar to those of three-phase machines, and they can be roughly classified in electrical (e.g., stator short-circuit fault), mechanical (e.g., bearing damage and rotor eccentricity), and magnetic faults (e.g., magnet damage/demagnetization). Partial short circuit is one of the most critical. If it occurs on a small number of turns of a phase winding (interturn short circuit), the inductance is very low and only the resistance limits the short-circuit current; therefore,

a quick detection of the fault is highly appreciated to avoid damage progression and catastrophic failure.

A fault causes an asymmetry in the machine, producing an electrical signature that can be detected by noninvasive techniques based on time-domain analysis, frequency analysis, or time–frequency analysis of different physical quantities [21], [22]. The most common technique, motor current signature analysis (MCSA), is based on the analysis of the harmonic content of the stator currents. The spectrum of the currents contains information (i.e., signatures) related to the presence of electrical and/or mechanical faults and can even permit a quantitative analysis of damage progression [23]. A general approach for the diagnosis of stator asymmetries in a multiphase drive was presented in [24]. Other papers in the literature investigated the effects of faults in multiphase motor drives, including short-circuit and open-circuit faults, and proposing methods to bypass the faulted components and techniques to increase the reliability of the drive [25]–[30]. In [31], a diagnostic method based on MCSA coupled with zero-sequence voltage analysis was applied to a five-phase PM machine with independent winding, together with a detailed analysis of machine power losses under fault conditions, carried out by FE simulations.

This paper is based upon the fault detection index described in [32] that relies on the combination of information from two different reference frames giving a dc component ideally equal to zero in healthy condition and different from zero during a fault (with a value proportional to damage severity). To improve fault recognition, the technique is further developed here. The diagnostic technique proposed here is based on the analysis of the whole spectrum of the combined space vector $\vec{D}$ rather than the D_0 dc component alone with the particular aim of enhancing the robustness of interturn fault detection. The robustness of interturn fault detection against other fault types is evaluated by means of FE analysis. The proposed technique for interturn fault detection is then experimentally assessed on a reference machine at different operating points and fault severity levels. The aim is to develop a reliable fault classification procedure that is capable of an early detection of interturn short-circuit faults in multiphase machines and is capable of differentiating interturn faults among other types of faults.

The proposed technique is an online and noninvasive method, which uses the measured voltage or current for each phase to construct the combined space vector. It can be implemented in an existing electric drive as it does not require any dedicated/additional transducer for the fault detection.

The main drawback is that a measurement of the currents (for a voltage source inverter drive) or the voltage (for a current source inverter drive) of each phase is required. Moreover, a dedicated power converter having suitable architecture and multiphase output must be developed [33]–[36].

The diagnostic index and proposed method are aimed at the detection of interturn short-circuit faults. The detection of this kind of fault is challenging since the distortion of the flux is of modest entity and the asymmetry is very small (particularly in case of a low number of short-circuited turns, i.e., the worst case scenario), although the short-circuit current is high [37]. Section III details the combined reference frame construction for the diagnostic purposes and the proposed fault detection, based on the combined space-vector spectrum analysis. Section IV presents a preliminary assessment of the robustness of the proposed method against different faults that cause machine imbalance (e.g., rotor eccentricities and magnet damage). Section V presents the proposed implementation of the diagnostic technique, applied to a current-controlled voltage source inverter (CCVSI) electric drive. Since the classic field-oriented control (FOC) imposes sinusoidal currents (thus masking the fault signatures), the proposed technique is applied to voltage quantities, particularly the machine's phase voltages. Section VI reports the experimental results on a prototype machine operated at different speed and load levels and increasing fault severity.

II. Combined Space Vector $\vec{D}$ for Interturn Short-Circuit Detection

A. Construction of the Combined Space Vector

The effect of an interturn short circuit is analyzed using the symmetrical component transformation in [4], [38]. The transformation from phase components to orthogonal components can be obtained with different variations. For the construction of the combined space vector, the same transformation used in [38] was used in

$$\begin{bmatrix} v_\alpha \\ v_\beta \\ v_{\alpha_2} \\ v_{\beta_2} \\ v_0 \end{bmatrix} = K \begin{bmatrix} \mathfrak{Re}(\dot{a}^0 & \dot{a}^1 & \dot{a}^2 & \dot{a}^3 & \dot{a}^4) \\ \mathfrak{Im}(\dot{a}^0 & \dot{a}^1 & \dot{a}^2 & \dot{a}^3 & \dot{a}^4) \\ \mathfrak{Re}(\dot{a}^0 & \dot{a}^2 & \dot{a}^4 & \dot{a}^6 & \dot{a}^8) \\ \mathfrak{Im}(\dot{a}^0 & \dot{a}^2 & \dot{a}^4 & \dot{a}^6 & \dot{a}^8) \\ \frac{1}{\sqrt{2}} & \frac{1}{\sqrt{2}} & \frac{1}{\sqrt{2}} & \frac{1}{\sqrt{2}} & \frac{1}{\sqrt{2}} \end{bmatrix} \begin{bmatrix} v_a \\ v_b \\ v_c \\ v_d \\ v_e \end{bmatrix} \quad (1)$$

where $\dot{a} = e^{j2\pi/5}$, and $K = 2/5$ was chosen for transformation with constant amplitude. The first two components define the space vector $\vec{v}_{\alpha\beta} = v_\alpha + jv_\beta$, whereas the third and fourth components define the space vector $\vec{v}_{\alpha_2\beta_2} = v_{\alpha_2} + jv_{\beta_2}$. As reported in [32], $\vec{v}_{\alpha\beta}$ presents only the harmonics of order $\nu = \pm 1 \pm 5k$, with $k = 0, \pm 1, \pm 2, \ldots$, whereas $\vec{v}_{\alpha_2\beta_2}$ presents only the harmonics of order $\nu = \pm 2 \pm 5k$, with $k = 0, \pm 1, \pm 2, \ldots$.

In order to avoid information loss, a combination of $\vec{v}_{\alpha\beta}$ and $\vec{v}_{\alpha_2\beta_2}$ can be useful to maximize the harmonics variation from healthy to faulty machine. In this paper, the combined space vector used for diagnostic purposes is defined as

$$\vec{D} = \vec{v}_{\alpha\beta} \cdot \vec{v}_{\alpha_2\beta_2}. \quad (2)$$

The following section describes the effectiveness of the $\vec{D}$ spectrum to provide a clear reliable interturn fault signature characterized by the increase in two different harmonics. Section III highlights its robustness with respect to other types of faults. In the experimental results, the diagnostic performance of the analysis of $\vec{D}$ spectrum was compared against that of the traditional $\vec{v}_{\alpha\beta}$ spectrum.

B. Application of $\vec{D}$ to Interturn Short-Circuit Detection

This section details the effectiveness of the combined space vector $\vec{D}$ spectrum analysis applied to interturn fault detection.

It is based on a simple model of the effects of the interturn short-circuit fault on the machine's back electromotive force (EMF). The same effects appear to the voltages applied to every phase when sinusoidal currents are imposed by a CCVSI [24]. Under these operating conditions, it is assumed that an interturn short-circuit fault, which occurs in one phase coil, affects only the amplitudes of voltage [32]. Defining the voltage reduction factor κ $(0 < \kappa < 1)$ inside the expressions of phase voltages and considering only one harmonic (the harmonic of νth order), the faulty phase voltage is expressed by the real part of

$$\kappa V_\nu e^{\jmath(\nu\omega t+\varphi_\nu)} \tag{3}$$

whereas the space vector $\vec{v}_{\alpha\beta}$ becomes

$$\vec{v}_{\nu\alpha\beta,a'} = \kappa V_\nu e^{\jmath(\nu\omega t+\varphi_\nu)} + \sum_{h=1}^{4} V_\nu e^{\jmath\left(\nu\omega t+\varphi_\nu+(1-\nu)h\frac{2\pi}{5}\right)}. \tag{4}$$

Subscript a' in the space vector of (4) means that the interturn fault arises in phase a. The first addendum can be split in

$$\kappa V_\nu e^{\jmath(\nu\omega t+\varphi_\nu)} = \left[V_\nu + V_\nu(\kappa-1)\right] e^{\jmath(\nu\omega t+\varphi_\nu)} \tag{5}$$

isolating the healthy-phase voltage component. Therefore, the difference between the healthy- and the faulty-phase voltage signals corresponds to the quantity $V_\nu(\kappa-1)e^{\jmath(\nu\omega t+\varphi_\nu)}$.

In the event of a fault, all the harmonic components could appear in the spectrum, whereas in the healthy case, only harmonics at $\nu = \pm 1 \pm 5k$ would appear [28].

The interturn short circuit can be then detected by checking the additional harmonics and because their amplitude decreases with ν. The most effective detection of this fault using the fast Fourier transform of $\vec{v}_{\alpha\beta}$ is to analyze the increase in the negative fundamental component $-f_s$: This procedure is the traditional MCSA methodology used to identify stator asymmetries in three-phase machines.

In the same way, considering only the fundamental component, the space vector $\vec{v}_{\alpha_2\beta_2}$ results in

$$\vec{v}_{\alpha_2\beta_2,a'} = (\kappa-1)V\cos(\omega t)e^{(\jmath 0)} \tag{6}$$

where the remaining part is equal to zero.

In general, if such perturbation occurs in the hth phase, the space vector becomes

$$\vec{v}_{\alpha_2\beta_2,h'} = (\kappa-1)V\cos\left(\omega t - h\frac{2\pi}{5}\right)e^{(\jmath h\frac{4\pi}{5})}. \tag{7}$$

The result of (7) is a pulsating vector along a particular direction that can be used to identify the faulty phase [24].

Continuing to consider at first only the fundamental component, in case of a fault in one phase winding, the multiplication of the two space vectors as defined in (2) determines the presence of three components in the spectrum of the combined reference frame $\vec{D}$. Fig. 1 shows the effects of the multiplication of the two harmonics of every space vector in case of an attenuation of 10% of the phase a.

In the spectrum of $\vec{D}$, the components that identify the fault are the dc component D_0 and the $2f_s$ component at twice the fundamental supply frequency. These two components are the best candidates for stator fault identification.

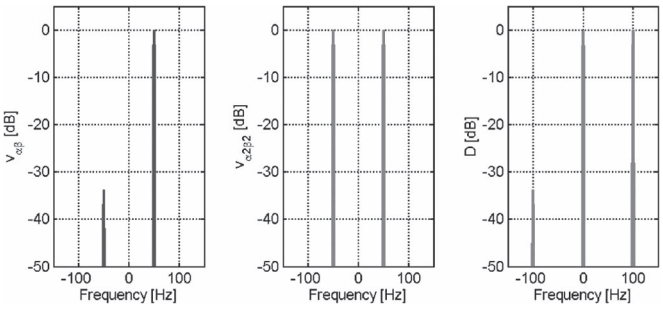

Fig. 1. Space vector of a machine with interturn short circuit. (From left to right) Spectra of $\vec{v}_{\alpha\beta}$ and $\vec{v}_{\alpha 2\beta 2}$ and $\vec{D}$ spectra considering only the fundamental component. The fault was modeled with a 10% attenuation of the faulty phase "a" amplitude.

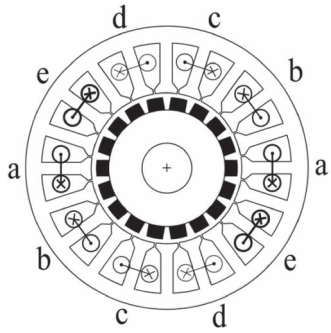

Fig. 2. Machine geometry and windings layout of the PM five-phase machine used for FEM simulation and experimental prototype.

The presence of all the harmonics of actual phase voltages was analyzed in [32]. In that work, it was shown as the presence of all the harmonics determine an increase in the dc component of $\vec{D}$ spectrum, i.e., D_0.

However, the greatest contribution to D_0 is caused by the unbalance of the fundamental component in the five phases of the machine. Therefore, in case of interturn short-circuit fault, the second harmonic of fundamental supply frequency $2f_s$ in the $\vec{D}$ spectrum results of comparable amplitude. Therefore, the simultaneous presence of a significant increase in the latter harmonic can be used to identify the interturn short-circuit fault with respect to other types of faults. This consideration was validated using FE analysis and experimental results on a reference five-phase machine.

III. Preliminary Analysis of Different Fault Conditions

A preliminary investigation of the proposed methodology applied to the reference machine is carried out by means of FE analysis. Moreover, at this stage, the robustness of interturn fault detection against other types of faults is evaluated. Modeling of the machine under normal and faulty conditions is done by means of 2-D FE analysis using FE method (FEM) magnetics (FEMM) software and dedicated scripts (see Fig. 2). All parameters for FE analysis were obtained from the experimental prototype used for the experiments (see Table I). The linkage flux and back EMF during healthy and faulty conditions were

TABLE I
REFERENCE MACHINE PARAMETERS

Symbol	Description	Value	Unit of Measurement
$2p$	Number of poles	18	
R_f	Phase Resistance	23.6	Ω
L_f	Phase Inductance	82	mH
m	Number turns per phase	692	
m	Number of Phases	5	
Q_s	Number of Slots	20	
D_e	External Diameter	120	mm
D_g	Gap Diameter	70	mm
L_g	Air gap Length (nominal)	0.5	mm
L	Stack Length	50	mm
I_n	Rated Current	0.6	A_{rms}
n_n	Nominal Speed	333	rpm
T_n	Nominal Torque	5.5	Nm
P_n	Rated Power	200	W

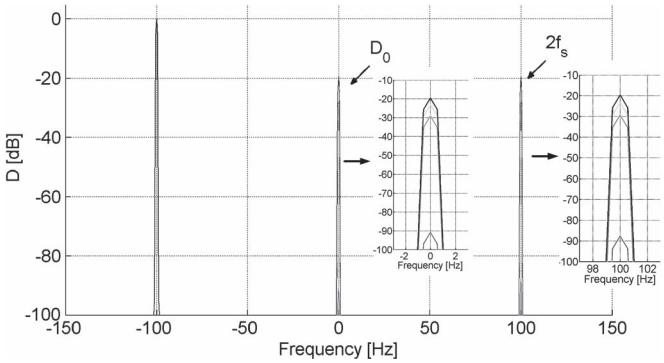

Fig. 3. Combined space vector $\vec{D}$ computed from FEM simulations under different levels of short circuit. (Blue) Healthy machine. (Red) 3% of short-circuited turns. (Green) 6% of short-circuited turns. (Black) 9% of short-circuited turns.

computed from FEMM results for each case. For all the simulations, the combined space vector $\vec{D}$ was computed from the phase voltages at no-load condition and nominal speed (333 r/min), corresponding to a fundamental frequency f_s of 50 Hz.

The interturn short-circuit fault on one winding coil was modeled according to [28]. Fig. 3 shows the $\vec{D}$ spectrum for the healthy machine, and at increasing level of interturn short-circuit (3%, 6%, and 9% shorted-winding turns, respectively).

As shown in Fig. 3, the effect of the interturn fault on D_0 and $2f_s$ components of the combined reference frame can be advantageously exploited to correctly identify this fault from other faults, as will be discussed in the following. From the healthy machine to minimum fault severity, i.e., 3% of short-circuited turns, a very large variation of D_0 and $2f_s$ components is visible. Because of the intrinsic asymmetries of the stator winding of an actual machine, this strong amplitude variation is expected to be reduced; in particular, the amplitudes of D_0 and $2f_s$ are expected to increase in the healthy machine as well.

In addition to the interturn fault detection, which is the topic of this paper, the analysis comprises three other faults presented as case studies, namely, partial magnet demagnetization and static and dynamic eccentricity. To model machine eccentricity [16], the rotor axis was offset by 0.25 mm to impose a 50% air-gap eccentricity on the machine. Both conditions resulted in an unbalanced field distribution inside the machine. For static eccentricity, during simulation, the rotor was turned around its axis, resulting in an unbalanced field distribution stationary

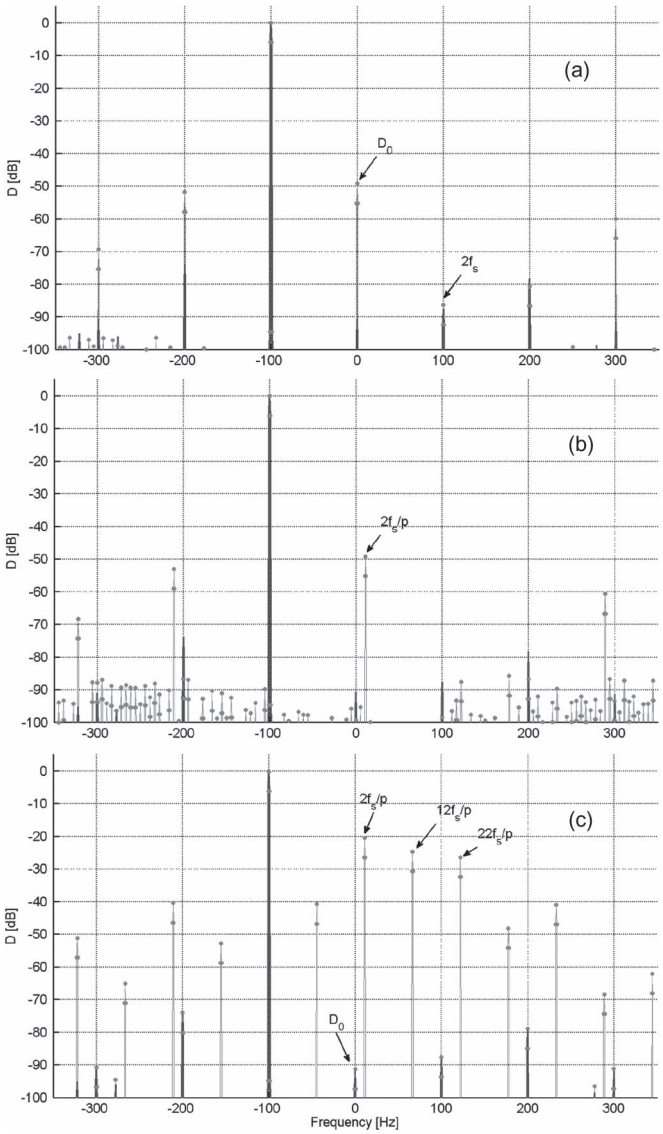

Fig. 4. Combined space vector $\vec{D}$ spectrum, computed from FEM simulations of different fault cases, starting from the top. (a) Static eccentricity. (b) Dynamic eccentricity. (c) Partial demagnetization. (Blue) healthy machine. (Red) Faulty machine.

with respect to the stator. For dynamic eccentricity, the rotor was turned around the stator axis, resulting in an unbalanced field distribution rotating together with the rotor. To simulate the case of a damage to the rotor's magnets (either break or demagnetization), the residual magnetization of a single magnet was reduced by 30%.

Fig. 4 shows the combined space vector $\vec{D}$ spectra in case of these other unbalancing faults.

In $\vec{D}$, the fundamental harmonic component at -100 Hz $(-2f_s)$ results from the combination of the primitive space vectors' fundamental components: 50 Hz f_s for $v_{\alpha\beta}\vec{}$ and -150 Hz for $v_{\alpha 2\beta 2}\vec{}$. The other harmonic components in $\vec{D}$ spectra arise from the multiplication of the all harmonic components of space vectors $v_{\alpha\beta}\vec{}$ and $v_{\alpha 2\beta 2}\vec{}$ [see (2)].

As can be seen, the results show that the different faults are characterized by different signatures in the combined space vector.

- Static eccentricity causes an increase in D_0 but not in $2f_s$.

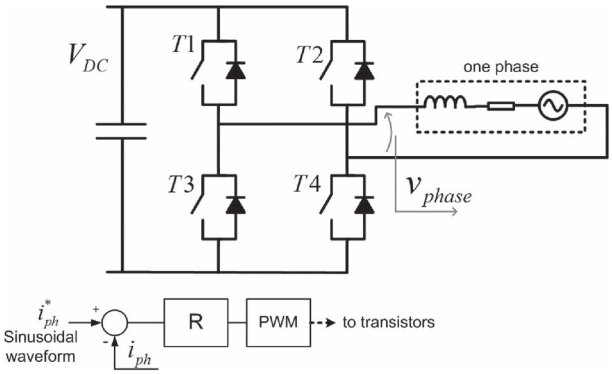

Fig. 5. Example of fault-tolerant electric drive architecture. One phase shown, together with dedicated H-bridge.

- Dynamic eccentricity does not affect either D_0 or $2f_s$. A component at $2f_s/p$ is present and is consistent with the eccentricity characteristic harmonics [21].
- Partial demagnetization fault does not affect either D_0 or $2f_s$. A component at $2f_s/p$ is present, together with the upper harmonics $12f_s/p$ etc.

For instance, the harmonic component $2f_s/p$ arises in the $\vec{D}$ spectrum in case of faults causing amplitude modulation in all phases: dynamic eccentricity [39] and partial demagnetization. In the latter case, the higher order harmonics are spaced by $10f_s/P$, as in [40].

IV. Proposed Application to a Fault-Tolerant Electric Drive

A multiphase fault-tolerant electric drive must continue to operate in case of first fault and, in some applications, also in the presence of a second one. The fault-tolerant capability can be maximized by employing an electric machine characterized by a null mutual inductance between phases in conjunction with a power electronics capable of controlling each phase independently, e.g., with independent H-bridges for every phase. The configuration is shown in Fig. 5 where a current control loop imposes a sinusoidal current for every phase. In this scenario, the proposed diagnostic procedure exploits the phase voltages imposed by the H-bridges. It is worth noting that the proposed diagnostic procedure can be also applied to electric drives based on a single five-phase full bridge.

A reference machine geometry was employed for fault modeling, simulation, and experiments: It is a five-phase PM machine designed for fault-tolerant applications that is characterized by a mutual inductance equal to zero and a high self-inductance in order to limit the short-circuit current. Each stator coil is wound around a single tooth, achieving a single-layer winding with nonoverlapped coils [10]. Table I summarizes the characteristic parameters of the reference machine used in the simulation and experimental tests.

V. Experimental Results

A prototype of the five-phase PM machine with 20 slots and 9 pole pairs was built for the experimental tests (see Fig. 6). New windings were installed, and one phase winding was center-tapped with multiple taps to vary the fault severity by changing the number of short-circuited turns and allow interturn fault emulation (see Fig. 7).

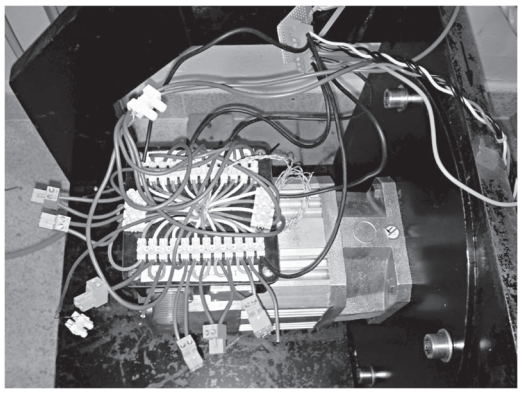

Fig. 6. Five-phase machine on the test bench, showing the center-tapped winding connections.

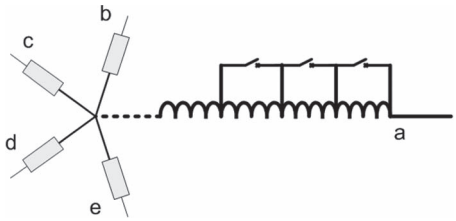

Fig. 7. Electric schematic of the five-phase machine detailing the center-tapped winding to emulate partial interturn short-circuit faults during operation.

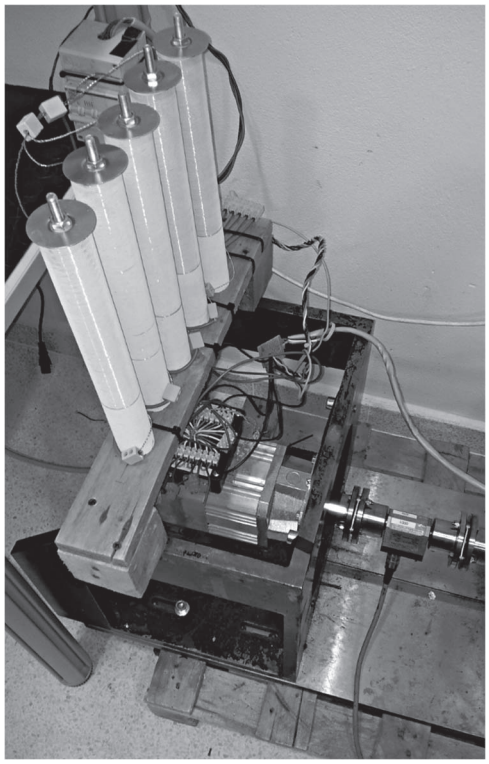

Fig. 8. Experimental test setup with resistive load.

The machine was mounted on a test bench and was operated as a generator (see Fig. 8). The test bench prime mover is an induction machine controlled by an FOC. The phase voltages were acquired at different speeds and different fault severity

TABLE II
TEST CONDITIONS

Test variable	Values	Unit of Measurement
$Speed$	100; 300	RPM
R_{load}	0; 250	Ω
$Fault\ severity$	0 $(healthy)$; 20; 60	$Short-circuited\ turns$

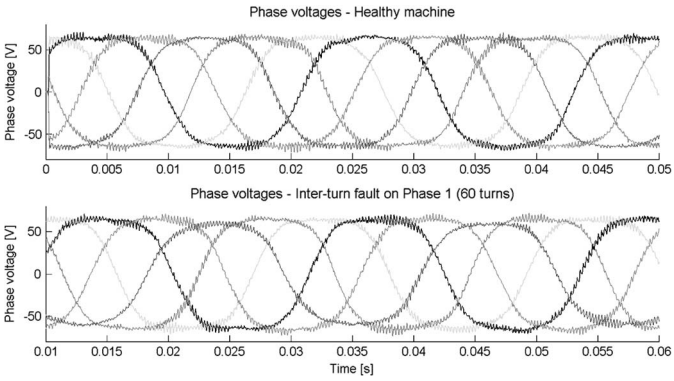

Fig. 9. Phase voltage waveforms in the healthy case and in the case of a 60-turn interturn fault. Machine is operated at 300 r/min and 250 Ω load.

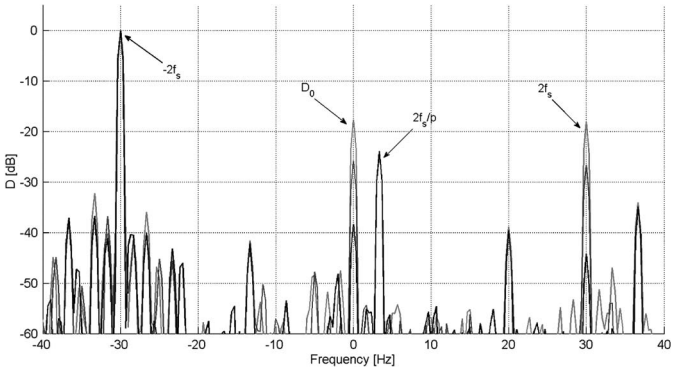

Fig. 10. Combined space vector $\vec{D}$ spectrum, computed from experimental acquisitions. Machine is operated at 100 r/min, no load, and increasing interturn fault severity: (black) healthy machine, (blue) 3% of short-circuited turns, and (red) 9% of short-circuited turns.

levels using a NI SignalExpress data logger composed by NI 9201 12-bit ADC modules on a CompactDAQ platform. The sample frequency was set to 100 kHz, with an acquisition time equal to 5 s for each test run.

The machine was run at a constant speed of 100 and 300 r/min and increasing numbers of coils were short circuited: starting from healthy machine, up to 60 short-circuited turns, corresponding respectively, to 9% of the total winding turns. Table II summarizes the test conditions. To test the machine under load, the output was connected to a load composed by five 250-Ω power resistors. To avoid destroying the auxiliary windings used for emulating the interturn faults, the tests were conducted at reduced power, limited to half the rated power of the machine.

The phase voltages were acquired and then postprocessed in MATLAB environment to obtain the proposed combined reference frame. Fig. 9 shows the phase voltages of the machine in the healthy case and with a 60-turn interturn fault on Phase 1.

Figs. 10–13 show the results of the proposed method for the machine running with different fault levels: (black) healthy machine, (blue) 3% of short-circuited turns, and (red) 9% of

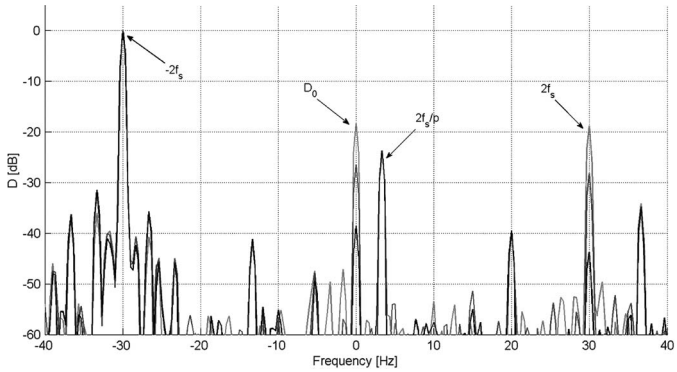

Fig. 11. Combined space vector $\vec{D}$ spectrum, computed from experimental acquisitions. Machine is operated at 100 r/min, 250-Ω load, and increasing interturn fault severity: (black) healthy machine, (blue) 3% of short-circuited turns, and (red) 9% of the short-circuited turns.

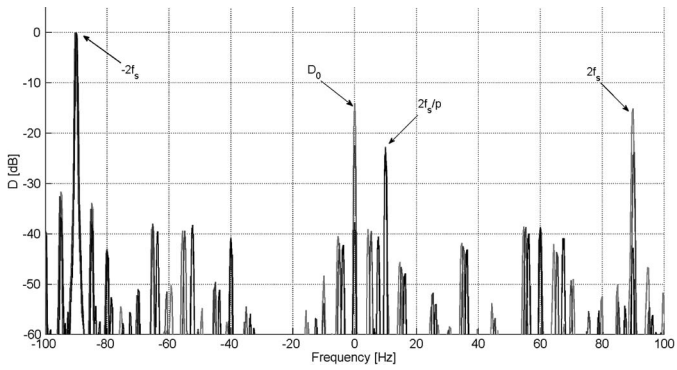

Fig. 12. Combined space vector $\vec{D}$ spectrum, computed from experimental acquisitions. Machine is operated at 300 r/min, no load, and increasing interturn fault severity: (black) healthy machine, (blue) 3% of short-circuited turns, and (red) 9% of short-circuited turns.

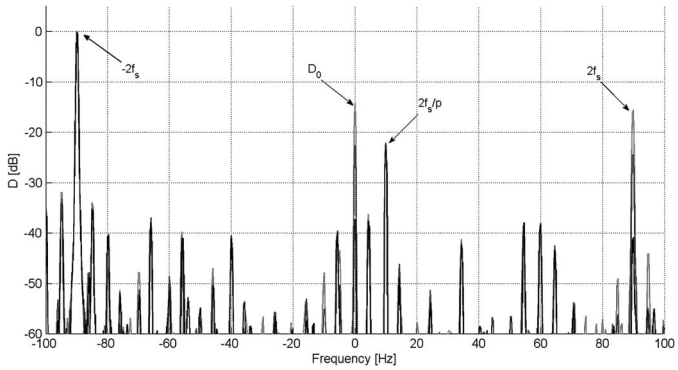

Fig. 13. Combined space vector $\vec{D}$ spectrum, computed from experimental acquisitions. Machine is operated at 300 r/min, 250-Ω load, and increasing interturn fault severity: (black) healthy machine, (blue) 3% of short-circuited turns, and (red) 9% of short-circuited turns.

short-circuited turns. Figs. 10 and 11 show the combined space vector $\vec{D}$ spectra for the machine operating at 100 r/min at no load and with 250-Ω resistive load, respectively.

Figs. 12 and 13 show the combined space vector $\vec{D}$ spectra for the machine operating at 300 r/min at no load and with 250-Ω resistive load, respectively. In all the test runs, the combined reference frame allowed to clearly identify the unbalance caused by the interturn fault, with an amplitude increase in the affected harmonics of more than 25 dB from the healthy case up to the maximum-fault-severity case.

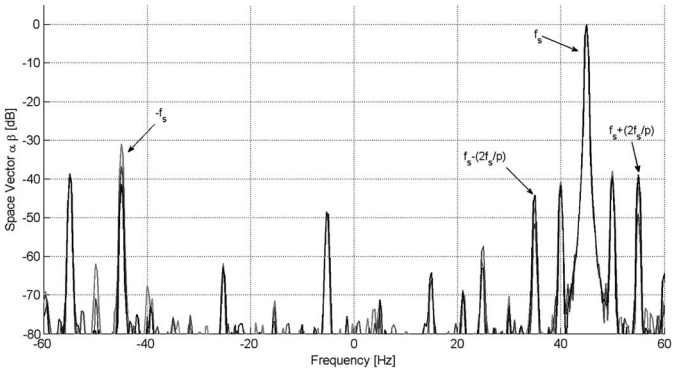

Fig. 14. $v_{\alpha\beta}$ space-vector spectrum, computed from experimental acquisitions. Machine is operated at 300 r/min, 250-Ω load, and increasing interturn fault severity: (black) healthy machine, (blue) 3% of short-circuited turns, and (red) 9% of short-circuited turns.

It is important to put in evidence that, in addition to the interturn short-circuit fault, other unbalances in the machine can alter the fault signature frequency components but with a different amplitude pattern, e.g., different amplitude ratio between zero frequency component D_0 and the $2f_s$ component. The influence of other operating conditions such as asymmetric power flow (e.g., due to electric drive malfunctioning or fault compensation algorithm) will be addressed in a future research.

To give a comparison, Fig. 14 shows the results obtained by analyzing the traditional space-vector spectrum computed on a single reference frame $\alpha\beta$. From the healthy to the maximum fault severity, a 10-dB increase in the negative sequence can be seen, together with the characteristic supply frequency sidebands due to an inherent imbalance of the machine. The experimental $\vec{v}\alpha\beta$ spectrum shown is for a single operating condition, but same results were obtained for the other operating conditions shown for $\vec{D}$ spectra. By comparing this result against the proposed method, it can be seen that the combined reference frame representation is much richer and sensitive.

The fixed amplitude $2f_s/p$ harmonic appearing in all the combined space vector $\vec{D}$ spectra (see Figs. 10–13) testifies an inherent imbalance of the machine used in the experiments, probably related to construction tolerances. Again, the proposed method allows directly identifying the fault signature harmonics, instead of analyzing sidebands on the fundamental. The results are consistent with the one obtained by FEM simulations of the fault case studies.

VI. Conclusion

A diagnostic procedure that merges information from two different reference frames (i.e., $\alpha\beta$ and $\alpha_2\beta_2$) into a combined space vector $\vec{D}$ has been developed and applied to the case of a five-phase PM machine. The proposed method allows to reliably detect interturn short-circuit faults and is capable of discriminating them from other unbalancing faults.

The reference machine geometry employed for fault modeling, simulation, and experiments is a five-phase PM machine designed for fault-tolerant applications that is characterized by a mutual inductance equal to zero and a high self-inductance in order to limit the short-circuit current.

Results show that the interturn short-circuit fault can be efficiently detected by monitoring the amplitude of D_0 and $2f_s$ components of the combined space vector $\vec{D}$, whose amplitude is greatly increased in the event of said fault.

The proposed combined reference frame representation is much richer and sensitive than the traditional single reference frame space-vector analysis. The combined space vector allows to clearly identify the unbalance caused by the interturn fault, with an amplitude increase in the affected harmonics by more than 25 dB from the healthy case to the maximum fault severity, which was experimentally observed.

By using the harmonic content information of the combined reference frame, the faults can be precisely detected, and the results show that the proposed method is robust and able to distinguish interturn short-circuit fault from other fault types (e.g., rotor eccentricities and rotor demagnetization), thus avoiding false positive detection.

The experimental results agree with the ones obtained from simulations. The main difference being the increase in the baseline fault signature values of the healthy machine in the $\vec{D}$ spectrum of the experimental results with respect to the simulation results. This is caused by the inherent construction asymmetries already present in the healthy physical machine, further demonstrating the robustness of the proposed method.

Acknowledgment

The authors would like to thank the Department of Electrical Engineering, University of Padua, Padua, Italy, and particularly Prof. N. Bianchi for providing the prototype of the machine that was rewound and employed in the experiments.

References

[1] L. Parsa, "On advantages of multi-phase machines," in *Proc. IEEE IECON*, 2005, pp. 1–6.
[2] E. Levi, "Multiphase electric machines for variable-speed applications," *IEEE Trans. Ind. Electron.*, vol. 55, no. 5, pp. 1893–1909, May 2008.
[3] A. Cavagnino, Z. Li, A. Tenconi, and S. Vaschetto, "Integrated generator for more electric engine: Design and testing of a scaled size prototype," *IEEE Trans. Ind. Appl.*, vol. 49, no. 5, pp. 2034–2043, Sep./Oct. 2013.
[4] L. Parsa and H. Toliyat, "Five-phase permanent-magnet motor drives," *IEEE Trans. Ind. Appl.*, vol. 41, no. 1, pp. 30–37, Jan./Feb. 2005.
[5] M. Villani, M. Tursini, G. Fabri, and L. Castellini, "High reliability permanent magnet brushless motor drive for aircraft application," *IEEE Trans. Ind. Electron.*, vol. 59, no. 5, pp. 2073–2081, May 2012.
[6] N. Bianchi, E. Fornasiero, and S. Bolognani, "Thermal analysis of a five-phase motor under faulty operations," *IEEE Trans. Ind. Appl.*, vol. 49, no. 4, pp. 1531–1538, Jul./Aug. 2013.
[7] N. Bianchi, S. Bolognani, and M. Pre, "Strategies for the fault-tolerant current control of a five-phase permanent-magnet motor," *IEEE Trans. Ind. Appl.*, vol. 43, no. 4, pp. 960–970, Jul./Aug. 2007.
[8] M. Kang, J. Huang, J. Yang, D. Liu, and H. Jiang, "Strategies for the fault-tolerant current control of a multiphase machine under open phase conditions," in *Proc. ICEMS*, 2009, pp. 1–6.
[9] R. Kianinezhad, B. Nahid-Mobarakeh, L. Baghli, F. Betin, and G.-A. Capolino, "Modeling and control of six-phase symmetrical induction machine under fault condition due to open phases," *IEEE Trans. Ind. Electron.*, vol. 55, no. 5, pp. 1966–1977, May 2008.
[10] N. Bianchi, S. Bolognani, and M. Pre, "Design and tests of a fault-tolerant five-phase permanent magnet motor," in *IEEE PESC*, 2006, pp. 1–8.
[11] M. El Hachemi Benbouzid, "A review of induction motors signature analysis as a medium for faults detection," *IEEE Trans. Ind. Electron.*, vol. 47, no. 5, pp. 984–993, Oct. 2000.

[12] S. Nandi, H. Toliyat, and X. Li, "Condition monitoring and fault diagnosis of electrical motors—A review," *IEEE Trans. Energy Convers.*, vol. 20, no. 4, pp. 719–729, Dec. 2005.
[13] A. Bellini, F. Filippetti, C. Tassoni, and G.-A. Capolino, "Advances in diagnostic techniques for induction machines," *IEEE Trans. Ind. Electron.*, vol. 55, no. 12, pp. 4109–4126, Dec. 2008.
[14] F. Immovilli, A. Bellini, R. Rubini, and C. Tassoni, "Diagnosis of bearing faults in induction machines by vibration or current signals: A critical comparison," *IEEE Trans. Ind. Appl.*, vol. 46, no. 4, pp. 1350–1359, Jul./Aug. 2010.
[15] M. Blodt, P. Granjon, B. Raison, and G. Rostaing, "Models for bearing damage detection in induction motors using stator current monitoring," *IEEE Trans. Ind. Electron.*, vol. 55, no. 4, pp. 1813–1822, Apr. 2008.
[16] J. Faiz, B.-M. Ebrahimi, B. Akin, and H. Toliyat, "Comprehensive eccentricity fault diagnosis in induction motors using finite element method," *IEEE Trans. Magn.*, vol. 45, no. 3, pp. 1764–1767, Mar. 2009.
[17] U. Kim and D. Lieu, "Magnetic field calculation in permanent magnet motors with rotor eccentricity: Without slotting effect," *IEEE Trans. Magn.*, vol. 34, no. 4, pp. 2243–2252, Jul. 1998.
[18] U. Kim and D. Lieu, "Magnetic field calculation in permanent magnet motors with rotor eccentricity: With slotting effect considered," *IEEE Trans. Magn.*, vol. 34, no. 4, pp. 2253–2266, Jul. 1998.
[19] B.-M. Ebrahimi, J. Faiz, and M. Roshtkhari, "Static-, dynamic-, mixed-eccentricity fault diagnoses in permanent-magnet synchronous motors," *IEEE Trans. Ind. Electron.*, vol. 56, no. 11, pp. 4727–4739, Nov. 2009.
[20] M. Mohr, O. Biro, A. Stermecki, and F. Diwoky, "An extended finite element based model approach for permanent magnet synchronous machines including rotor eccentricity," in *Proc. IEEE IECON*, Nov. 2013, pp. 2596–2601.
[21] P. Tavner, "Review of condition monitoring of rotating electrical machines," *IET Elect. Power Appl.*, vol. 2, no. 4, pp. 215–247, Jul. 2008.
[22] Y. Da, X. Shi, and M. Krishnamurthy, "A new approach to fault diagnostics for permanent magnet synchronous machines using electromagnetic signature analysis," *IEEE Trans. Power Electron.*, vol. 28, no. 8, pp. 4104–4112, Aug. 2013.
[23] W. le Roux, R. Harley, and T. Habetler, "Detecting rotor faults in low power permanent magnet synchronous machines," *IEEE Trans. Power Electron.*, vol. 22, no. 1, pp. 322–328, Jan. 2007.
[24] L. Zarri *et al.*, "Detection and localization of stator resistance dissymmetry based on multiple reference frame controllers in multiphase induction motor drives," *IEEE Trans. Ind. Electron.*, vol. 60, no. 8, pp. 3506–3518, Aug. 2013.
[25] L. Parsa and H. Toliyat, "Fault-tolerant five-phase permanent magnet motor drives," in *Conf. Rec. IEEE IAS Annu. Meeting*, 2004, vol. 2, pp. 1048–1054.
[26] C. Jacobina, I. Freitas, T. Oliveira, E. da Silva, and A. M. N. Lima, "Fault tolerant control of five-phase ac motor drive," in *IEEE PESC*, 2004, vol. 5, pp. 3486–3492.
[27] J. Apsley and S. Williamson, "Analysis of multiphase induction machines with winding faults," *IEEE Trans. Ind. Appl.*, vol. 42, no. 2, pp. 465–472, Mar./Apr. 2006.
[28] C. Bianchini, E. Fornasiero, T. Matzen, N. Bianchi, and A. Bellini, "Fault detection of a five-phase permanent-magnet machine," in *Proc. IEEE IECON*, 2008, pp. 1200–1205.
[29] H.-M. Ryu, J.-W. Kim, and S.-K. Sul, "Synchronous-frame current control of multiphase synchronous motor under asymmetric fault condition due to open phases," *IEEE Trans. Ind. Appl.*, vol. 42, no. 4, pp. 1062–1070, Jul./Aug. 2006.
[30] N. Bianchi, S. Bolognani, and M. Pre, "Impact of stator winding of a five-phase permanent-magnet motor on postfault operations," *IEEE Trans. Ind. Electron.*, vol. 55, no. 5, pp. 1978–1987, May 2008.
[31] H. Saavedra, J.-R. Riba, and L. Romeral, "Inter-turn fault detection in five-phase PMSMs. Effects of the fault severity," in *Proc. IEEE SDEMPED*, Aug. 2013, pp. 520–526.
[32] C. Bianchini, F. Immovilli, E. Lorenzani, A. Bellini, and E. Fornasiero, "Experimental evaluation of combined reference frames transformation for stator fault detection in multi-phase machines," in *Proc. IEEE SDEMPED*, Aug. 2013, pp. 491–496.
[33] R. Bojoi, M. G. Neacsu, and A. Tenconi, "Analysis and survey of multiphase power electronic converter topologies for the more electric aircraft applications," in *Proc. IEEE SPEEDAM*, 2012, pp. 440–445.
[34] O. Lopez, J. Alvarez, J. Doval-Gandoy, and F. Freijedo, "Multilevel multiphase space vector PWM algorithm," *IEEE Trans. Ind. Electron.*, vol. 55, no. 5, pp. 1933–1942, May 2008.
[35] D. Casadei *et al.*, "General modulation strategy for seven-phase inverters with independent control of multiple voltage space vectors," *IEEE Trans. Ind. Electron.*, vol. 55, no. 5, pp. 1921–1932, May 2008.
[36] L. De Lillo *et al.*, "Multiphase power converter drive for fault-tolerant machine development in aerospace applications," *IEEE Trans. Ind. Electron.*, vol. 57, no. 2, pp. 575–583, Feb. 2010.
[37] A. Gandhi, T. Corrigan, and L. Parsa, "Recent advances in modeling and online detection of stator interturn faults in electrical motors," *IEEE Trans. Ind. Electron.*, vol. 58, no. 5, pp. 1564–1575, May 2011.
[38] E. Levi, M. Jones, S. Vukosavic, A. Iqbal, and H. Toliyat, "Modeling, control, experimental investigation of a five-phase series-connected two-motor drive with single inverter supply," *IEEE Trans. Ind. Electron.*, vol. 54, no. 3, pp. 1504–1516, Jun. 2007.
[39] B. Ebrahimi, M. Javan Roshtkhari, J. Faiz, and S. Khatami, "Advanced eccentricity fault recognition in permanent magnet synchronous motors using stator current signature analysis," *IEEE Trans. Ind. Electron.*, vol. 61, no. 4, pp. 2041–2052, Apr. 2014.
[40] D. Casadei *et al.*, "Detection of magnet demagnetization in five-phase surface-mounted permanent magnet generators," in *Proc. IEEE PEDG*, Jun. 2012, pp. 841–848.

Fabio Immovilli (S'08–M'11) was born in Italy on March 11, 1981. He received the M.S. and Ph.D. degrees in mechatronic engineering from the University of Modena and Reggio Emilia, Reggio Emilia, Italy, in 2006 and 2011, respectively.

In 2009, he was a Visiting Scholar with the Power Electronics, Machines and Control Group, The University of Nottingham, Nottingham, U.K. Since 2011, he has been with the University of Modena and Reggio Emilia, where he joined as a Research Fellow in electric converters, machines, and drives the Department of Sciences and Methods for Engineering. He holds one international industrial patent. His research interests include electric machine diagnosis, power converters, machines for energy conversion from renewable energy sources, and thermoacoustics.

Dr. Immovilli is a member of the Italian Association of Converters, Electrical Machines and Drives (CMAEL).

Claudio Bianchini (S'08–M'10) was born in Italy on September 9, 1974. He received the M.S. degree in management engineering, the S.B. degree in mechatronics, and the Ph.D. degree from the University of Modena and Reggio Emilia, Reggio Emilia, Italy, in 2002, 2006, and 2010, respectively.

During 2008, he was an Honorary Scholar with the University of Wisconsin-Madison, Madison, WI, USA. Since 2010, he has been with the University of Modena and Reggio Emilia, where he joined as a Research Fellow in electric converters, machines, and drives the Department of Sciences and Methods for Engineering. He is the holder two international patents. His research interests include electric machines and drives and static power conversion for renewable energy.

Emilio Lorenzani (S'03–M'07) was born in Parma, Italy, in 1976. He received the M.S. degree in electronic engineering and the Ph.D. degree in information technologies from the University of Parma, Parma, in 2002 and 2006, respectively.

Since 2011, he has been with the Department of Sciences and Methods for Engineering, University of Modena and Reggio Emilia, Reggio Emilia, Italy, where he is currently an Assistant Professor of electric machines and drives. He is the author or coauthor of more than 50 technical papers, and he is the holder of five industrial patents. His research activity is mainly focused on power electronics for renewable energy resources, electric drives, and electric motor diagnostics.

Dr. Lorenzani is a member of the Italian Association of Converters, Electrical Machines and Drives (CMAEL).

Alberto Bellini (S'96–M'99) was born in Italy in 1969. He received the M.S. degree in electronic engineering and the Ph.D. degree in computer science and electronics engineering from the University of Bologna, Bologna, Italy, in 1994 and 1998, respectively.

From 1999 to 2004, he was with the University of Parma, Parma, Italy. During 2000, he was an Honorary Scholar with the University of Wisconsin-Madison, Madison, WI, USA. From 2004 to 2013, he was with the University of Modena and Reggio Emilia, Reggio Emilia, Italy. Since 2013, he has been an Associate Professor of electric machines and drives with the University of Bologna. He is the author or coauthor of more than 90 papers and one textbook, and he is the holder of three industrial patents. His research interests include electric drive design and diagnosis, power electronics, and signal processing.

Dr. Bellini was the recipient of the First Prize Paper Award from the Electric Machines Committee of the IEEE Industry Applications Society in 2001.

Emanuele Fornasiero received the M.S. and Ph.D. degrees in electrical engineering from the University of Padova, Padua, Italy, in 2006 and 2010, respectively. During his Ph.D. studies, he worked on the analysis of rotor losses and fault-tolerant fractional-slot permanent-magnet machines.

He is currently a Research Assistant with the University of Padova. His research activities are concentrated on the analysis and design of permanent-magnet synchronous machines, particularly for large-power applications.